EASR

Engineering and Applied Science Research

Improving drying shrinkage and strength development of alkali-activated high-calcium fly ash using commercial-grade calcium sulfate as expansive additive

Chudapak Detphan[1)], Patthamawadee Kaeorawang[1)], Borwonrak Injorhor[1)], Khattiya Chompoovong[1)], Sakonwan Hanjitsuwan[2)], Tanakorn Phoo-ngernkham*[1)] and Prinya Chindaprasirt[3, 4)]

[1)]Sustainable Construction Material Technology Research Unit, Department of Civil Engineering, Faculty of Engineering and Architecture, Rajamangala University of Technology Isan, Nakhon Ratchasima 30000, Thailand
[2)]Program of Civil Technology, Faculty of Industrial Technology, Lampang Rajabhat University, Lampang 52100, Thailand
[3)]Sustainable Infrastructure Research and Development Center, Department of Civil Engineering, Faculty of Engineering, Khon Kaen University, Khon Kaen 40002, Thailand
[4)]Academy of Science, The Royal Society of Thailand, Bangkok 10300, Thailand

Abstract

The effect of using commercial-grade calcium sulfate (CS) in alkali-activated high-calcium fly ash (AAHFA) paste on the drying shrinkage and strength is reported. Five different fly ash (FA): CS ratios of 100:0, 97.5:2.5, 95:5, 92.5:7.5, and 90:10 were investigated. A constant Na_2SiO_3:10 M NaOH ratio of 1.0, liquid alkaline activator/binder (L/B) ratio of 0.40, and ambient curing temperature (~25 °C) were used for all mixes. The results clearly showed a reduction in the setting time for the AAHFA incorporating CS. The compressive strength of the AAHFA paste increased with increasing CS content up to an optimum level. In addition, the use of a mixture of FA and CS to produce AAHFA could improve its drying shrinkage. The use of 2.5% CS or 5% CS is recommended to realize significant improvements in both the drying shrinkage and strength development of AAHFA paste.

Keywords: Alkali-activated high-calcium fly ash, Commercial-grade calcium sulfate, Strength development, Shrinkage compensation

1. Introduction

Portland cement (PC) is the most widely used cement for construction work despite the amount of CO_2 released during its manufacturing. Naqi and Jang [1] reported that the manufacturing of PC results in high emission of CO_2: approximately 0.814 ton of CO_2 for every ton of PC. To solve this problem, many researchers [2, 3] have aimed to utilize industrial by-products in the concrete industry. For example, fly ash (FA) is used to replace PC for producing cement and concrete [2, 3]. Currently, new binding materials called alkali-activated materials (AAMs) are receiving increasing attention for use as binders in green concrete. A number of researchers [4-12] have demonstrated that AAM binders can provide advantages over PC.

AAM is a type of cement that incorporates industrial by-products activated with an alkaline solution [13]. The main reaction products within AAM binders can be divided into two categories [14]: high-calcium products based on calcium silicate hydrate (CSH) and/or calcium aluminum silicate hydrate (CASH) gels, and low-calcium products based on sodium aluminosilicate hydrate (NASH) gels. The high-calcium products can provide a higher strength development compared with low-calcium products under normal temperatures [15]. A high strength development under normal temperatures is very useful for the construction industry, especially for repair work. Alkali-activated binders containing a combination of CSH, CASH, and NASH could be used as high-performance materials for repair work [12, 16, 17]. For example, an AAM incorporating PC and calcium carbide residue (CCR) has been developed for use as an alternative repair material [12, 18]. It has been reported that the AAM with PC and CCR as additives is a good choice for repair work in terms of its high bond strength and cost-effectiveness. However, the drying shrinkage of the AAM paste made from fly ash (FA) was much larger than that of the AAM paste made from PC [18, 19], except under heat-cured conditions. Matalkah et al. [20] proposed that the high shrinkage was due to the large number of small gel pores within alkali-activated binders, which result in a higher capillary stress and larger drying shrinkage. This may be a limitation for using AAM as a repair material, although AAMs exhibit high bonding strength and excellent durability. To solve this problem, Hanjitsuwan et al. [16] used expansive additives to improve the drying shrinkage. They found that the use of expansive additives in the AAM binder could reduce the drying shrinkage by 25-30%. Moreover, Bakharev et al. [21] reported that both the autogenous and drying shrinkage were improved with the use of 6% gypsum in alkali-activated slag, resulting in ettringite formation. It should be noted that the ettringite formed acts as the expansive phase.

Therefore, this study aims to investigate the effect of using commercial-grade calcium sulfate (CS) in AAM binders on their drying shrinkage and strength development. The drying shrinkage and strength development of alkali-activated high-calcium fly ash (AAHFA) binders incorporating CS are examined.

*Corresponding author. Tel.: +66 4423 3000
Email address: Tanakorn.ph@rmuti.ac.th

2. Experiments and analysis

2.1 Materials

High-calcium FA from the Mae Moh power plant in northern Thailand was used as the raw material. Commercial-grade CS (Ca_2SO_4) was used as the expansive additive. The FA had a specific gravity, median particle size, and Blaine fineness of 2.65, 15.3 μm, and 4300 cm^2/g, respectively. Table 1 lists the chemical compositions of the FA and CS. The sum of $SiO_2 + Al_2O_3 + Fe_2O_3$ in the FA was 66.94%, and the CaO content was 21.41%. Thus, the FA was Class C according to ASTM C618-15 [22]. Scanning electron microscopy (SEM) and energy-dispersive X-ray spectroscopy (EDS) images of the CS are shows in Figure 1. The EDS analysis of CS indicated that it mainly consisted of CaO and SO_3, as also shown in the X-ray fluorescence (XRF) analysis.

Table 1 Chemical compositions of FA and CS (wt. %)

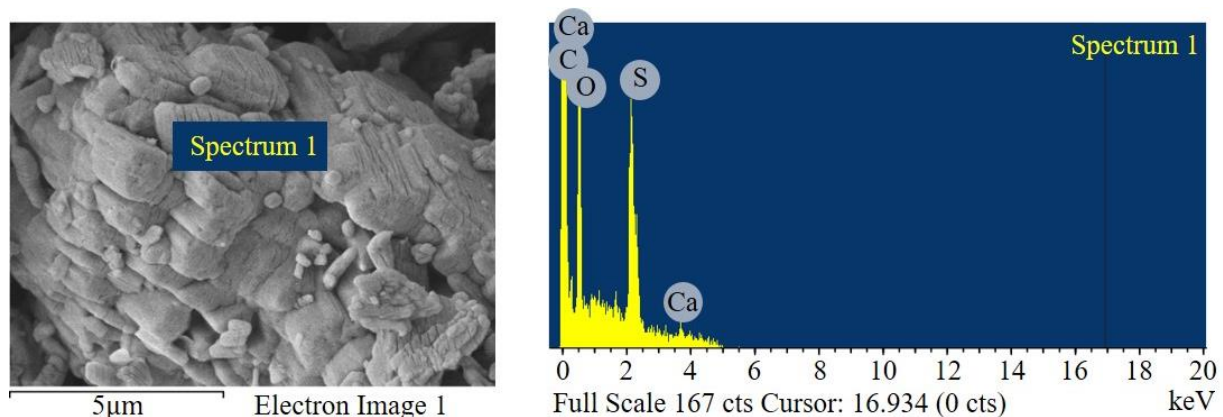| Material	SiO$_2$	Al$_2$O$_3$	Fe$_2$O$_3$	CaO	MgO	K$_2$O	Na$_2$O	TiO$_2$	P$_2$O$_5$	Other	SO$_3$	LOI
FA	36.94	18.11	11.90	21.40	2.79	2.29	1.43	0.37	0.21	0.15	2.89	1.52
CS	-	-	-	40.66	0.30	0.10	0.15	0.27	-	0.13	58.40	-

Figure 1 SEM and EDS images of CS

2.2 Mix proportions

Table 2 lists the mix proportions of the AAHFA pastes incorporating CS. The 10 M NaOH and Na_2SiO_3 solutions used in this study were based on a previous study [16]. The Na_2SiO_3/NaOH and L/B ratios were fixed at 1.0 and 0.40, respectively.

To obtain the paste, FA and CS were first dry mixed for 1 min to ensure homogeneity. Then, NaOH and Na_2SiO_3 were added, and the product was mixed for 2 min.

Table 2 Mix proportions of AAHFA pastes incorporating CS

Mix ID.	Symbol	FA (%)	CS (%)	10 M NaOH (%)	Na$_2$SiO$_3$ (%)
1	0CS	100	-	20	20
2	2.5CS	97.5	2.5	20	20
3	5.0CS	95.0	5.0	20	20
4	7.5CS	92.5	7.5	20	20
5	10CS	90.0	10.0	20	20

2.3 Testing procedure

After mixing, the setting times of the AAHFA pastes with CS were determined in accordance with ASTM C191-19 [23]. The compressive strength samples were obtained according to ASTM C109/C109M-20b [24]. Five identical samples were produced for each mix in a $50 \times 50 \times 50$ mm cubic mold. The samples were de-molded after 24 h and wrapped with a plastic sheet for 7, 14, 28, 60, 90, and 120 d of curing in a room at 25 ±2 °C.

For the shrinkage tests, three identical samples were produced for each mix in a $25 \times 25 \times 285$ mm prism mold according to ASTM C490/C490M-17 [25] and ASTM C596-18 [26]. After casting, the samples were kept at ambient temperature (~25 °C) and a relative humidity of 50% ±3% without a vinyl sheet. The measurement of the change in length of samples was based on a previous study [16]. Figure 2 shows the drying shrinkage test setup.

Figure 2 Drying shrinkage test setup

3. Results and discussion

3.1 Setting time

Figure 3 shows the results for the setting times of AAHFA pastes with varying CS contents. The initial and final setting times of samples 0CS, 2.5CS, 5CS, 7.5CS, and 10CS were 12, 7, 5, 5, and 2 min and 18, 13, 10, 9, and 3 min, respectively. The setting time of the AAHFA paste thus decreased with increasing CS replacement. This was due to the high Ca content from the CS, which was approximately 40.66%. This agrees with the conclusion reported by Pangdaeng et al. [27] that the reaction products within the AAM binder were accelerated by the heat generated from the exothermic process. CSH and/or CASH gels were formed in the matrix. This is also consistent with previous studies [28, 29]. These previous studies reported that the coexistence of CSH and NASH gels provided the high strength development of the AAM binders. It should be noted that the rapid setting of AAHFA with CS is advantageous for repair materials intended for projects such as repairing cracks and patch repair in ballastless track structures, asphalt pavement, and walkways, as reported by Wu et al. [30]. However, the fast setting of the AAHFA paste with CS may make it difficult to use in large areas. Thus, AAHFA with CS is recommended for use on only small areas of damaged concrete.
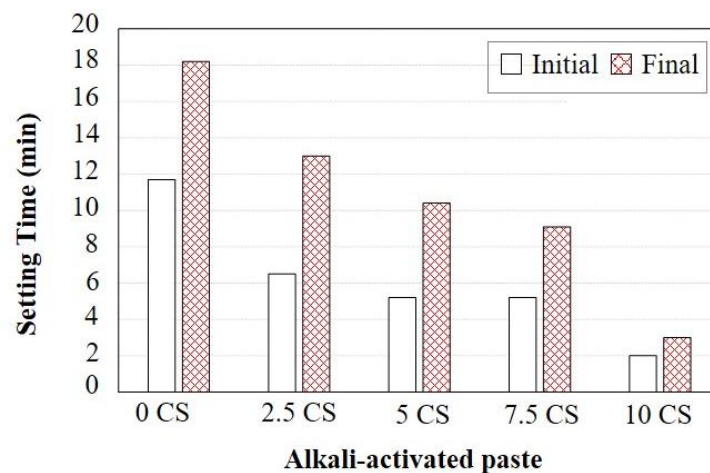

Figure 3 Setting times of AAHFA pastes incorporating CS

3.2 Compressive strength

Figure 4 shows the compressive strength of the AAHFA paste using CS as the expansive additive. The strength of the AAHFA paste tended to increase with increasing CS content up to an optimum level, after which the strength declined. For instance, the 28-d strengths of samples 0CS, 2.5CS, 5CS, and 7.5CS were 45.9, 51.2, 48.7, and 44.9 MPa, whereas the 120-d strengths were 58.0, 58.4, 54.3, and 51.9 MPa, respectively. Note that the setting time of the 10CS mix was very quick; therefore, there was not sufficient duration for sample preparation. The formation of CSH from FA and CS facilitated the high strength development of the AAHFA paste [16]. Punurai et al. [19] reported that the additional formation of CSH in the geopolymer system would refine its pore structure; hence, the strength development of the geopolymer was increased. Equation (1) shows the reaction mechanism between the gypsum and NaOH solution [31]. The Ca(OH)$_2$ obtained from Eq. (1) can react with SiO$_2$ and/or Al$_2$O$_3$ from the FA to form CSH [16]. In addition, the reaction of the SO_4^{2-} ions from Eq. (1) results in dissolution of the Al^{3+} ions from FA particles [32, 33], leading to strength development of the AAHFA paste. However, the Al^{3+} content in the matrix was reasonably high, which led to the formation of ettringite

($Ca_6Al_2(SO_4)_3(OH)_{12} \cdot 26H_2O$) and hence a reduction in strength. This behavior is confirmed in Figure 4. The 90-d strength of the AAHFA paste with 5% CS was lower than that of the AAHFA paste without CS.
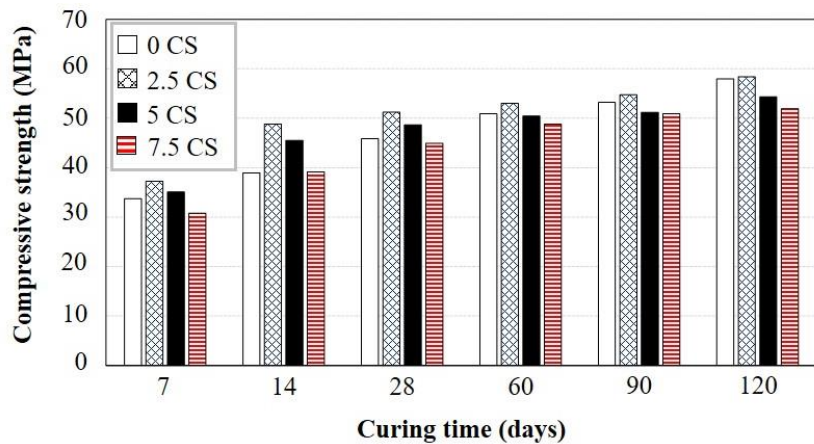
$$CaSO_4 2H_2O + NaOH \rightarrow 4Ca(OH)_2 + Na_2SO_4 \tag{1}$$

Figure 4 Compressive strengths of AAHFA pastes incorporating CS

3.3 Drying shrinkage

Figure 5 summarizes the results of the drying shrinkage tests of AAHFA pastes incorporating CS. The drying shrinkage decreased with increasing CS content compared to the paste without CS, as expected. For instance, the drying shrinkages at 90 d of curing were 12,076, 11,632, 8,169, and $7,391 \times 10^{-6}$ mm/mm for the 0CS, 2.5CS, 5CS, and 7.5CS mixes, respectively. This is consistent with the results of previous studies [19, 34], which reported high shrinkage values of AAM between $25,000 \times 10^{-6}$ and $30,000 \times 10^{-6}$ mm/mm. As reported, FA:CS ratios of 95:5 and 92.5:7.5 are optimal for improving the drying shrinkage. The CS acts as an expansive material, similar to the work of Hanjitsuwan et al. [16]. Gypsum and calcium sulfate hemihydrate were identified as the main components, as indicated in Table 1 and Figure 1. The formation of Na_2SO_4, obtained from Eq. (1) increased with increasing CS content. In addition, the formation of ettringite ($Ca_6Al_2(SO_4)_3(OH)_{12} \cdot 26H_2O$) had a positive effect on the shrinkage behavior of the AAM [16, 21, 31]. Bakharev et al. [21] demonstrated that the use of gypsum in AAM binders could enhance the drying shrinkage. It should be noted that the formation of ettringite and sodium sulfate are critical factors for obtaining low drying shrinkage values.
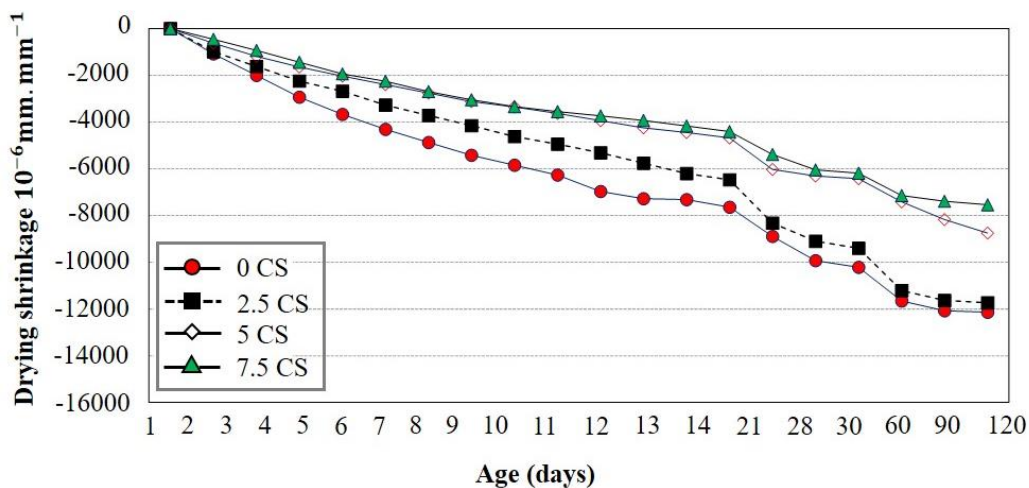

Figure 5 Effect of CS on the drying shrinkage of AAHFA pastes

3.4 SEM and EDS analysis

Figure 6 shows the microstructures of the AAHFA pastes incorporating CS. The SEM image of the alkali-activated FA paste without CS (Figure 6a) shows many unreacted FA particles in the matrix. For the mixes containing CS (Figure 6b and 6c), the SEM images appear denser with more closely packed reaction products than the paste without CS replacement, resulting in high strength development of the AAHFA pastes. However, the formation of ettringite was observed, as shown in Figure 6b and 6c. The occurrence of ettringite formation in the matrix could explain the reduction in the strength development of the AAHFA paste incorporating 5% CS at a curing age of 90 d (see Figure 4).

The main elements detected in the EDS analysis were similar to those reported by Hanjitsuwan et al. [16]. The presence of sodium, silicon, and aluminum represents the geopolymer gel in the AAHFA paste [16]. Similarly, the presence of calcium, silicon, and aluminum corresponds to the formation of C(A)SH gels. As shown in Figure 6, the Si/Al ratio is 1.51 for spectrum 1. For the pastes containing FA with 2.5% CS and 5% CS, the Si/Al ratios ranged between 1.47-3.03 and 1.24-2.87, respectively. High strength

development of the high-calcium AAM was always found at Si/Al ratios between 2.6 and 3.0, as reported in previous studies [19, 35]. In addition, the Ca/Si ratios of the pastes containing FA with 2.5% CS and 5% CS were 0.40-0.58 and 0.23-0.84, respectively. The Ca/Si ratio of approximately 1.0 represents the initial formation of CSH, as reported in previous studies [15, 36]. Therefore, the mixes with CS have a higher strength development than the mix without CS. However, a high amount of Al was found in Figure 6b and 6c; therefore, ettringite formation may have occurred (see Figure 6b). For spectra 1 and 3 in Figure 6a, a high amount of Al was detected, similar to the mixes with CS. In this case, the ettringite would not be formed because Ca was no longer present.

	Spectrum 1	Spectrum 2	Spectrum 3
(a) 0CS Element	Atomic (%)	Atomic (%)	Atomic (%)
O	62.64	60.04	52.10
Na	3.09	3.30	-
Mg	-	-	11.73
Al	11.04	-	9.12
Si	16.68	3.72	-
Ca	-	16.81	-
Fe	6.55	-	21.69
Si/Al	1.51	-	-
Ca/Si	-	4.52	-
Na/Al	0.03	-	-
	Spectrum 1	Spectrum 3	Spectrum 4
(b) 2.5CS Element	Atomic (%)	Atomic (%)	Atomic (%)
O	57.12	42.08	59.67
Na	1.92	6.58	1.88
Mg	-	-	-
Al	8.22	8.69	9.58
Si	15.85	26.37	14.06
Ca	6.61	15.39	5.62
Fe	1.63	0.89	3.07
Si/Al	1.93	3.03	1.47
Ca/Si	0.42	0.58	0.40
Na/Al	0.23	0.76	0.20
	Spectrum 1	Spectrum 2	Spectrum 3
(c) 5.0CS Element	Atomic (%)	Atomic (%)	Atomic (%)
O	52.86	51.77	35.79
Na	0.99	4.61	7.29
Mg	2.09	-	-
Al	7.03	6.55	12.56
Si	8.75	17.38	36.09
Ca	7.36	13.77	8.28
Fe	13.73	-	-
Si/Al	1.24	2.65	2.87
Ca/Si	0.84	0.79	0.23
Na/Al	0.14	0.70	0.58

Figure 6 Microstructures of AAHFA pastes incorporating CS at 90 days

4. Conclusions

From the results obtained in this study, the following conclusions can be drawn:

1. The AAHFA pastes with CS had reduced workability. The initial and final setting times ranged from 2-12 min and 3-18 min, respectively. The fast setting of the AAHFA paste with CS makes it difficult to use in large areas; therefore, it is recommended for use in only small areas of damaged concrete.

2. The strength development of the AAHFA paste increased with increasing CS replacement up to an optimum level. However, a reduction in the 90-d strength was observed in the AAHFA paste containing 5.0% CS. Therefore, the CS content of the AAHFA paste was an important factor in the strength development.

3. Using a mixture of FA and CS to produce the AAM could improve the drying shrinkage of the AAHFA pastes. The addition of 2.5% CS and 5% CS showed positive effects on both the drying shrinkage and strength development.

4. The use of CS in AAHFA pastes could improve the microstructure compared to the paste without CS. However, ettringite formation was observed in the pastes with CS. This led to a reduction in the strength development of the AAHFA paste incorporating 5% CS at the later stage despite the reduced drying shrinkage.

5. Acknowledgements

6. References

[1]   Naqi A, Jang JG. Recent progress in green cement technology utilizing low-carbon emission fuels and raw materials: a review. Sustainability. 2019;11(2):537.
[2]   Tangchirapat W, Buranasing R, Jaturapitakkul C. Use of high fineness of fly ash to improve properties of recycled aggregate concrete. J Mater Civ Eng. 2010;22(6):565-71.
[3]   Tangchirapat W, Jaturapitakkul C, Chindaprasirt P. Use of palm oil fuel ash as a supplementary cementitious material for producing high-strength concrete. Constr Build Mater. 2009;23(7):2641-6.
[4]   Puertas F, Palacios M, Manzano H, Dolado JS, Rico A, Rodriguez J. A model for the C-A-S-H gel formed in alkali-activated slag cements. J Eur Ceram Soc. 2011;31(12):2043-56.
[5]   Chindaprasirt P, Paisitsrisawat P, Rattanasak U. Strength and resistance to sulfate and sulfuric acid of ground fluidized bed combustion fly ash-silica fume alkali-activated composite. Adv Powder Tech. 2014;25(3):1087-93.
[6]   Hanjitsuwan S, Phoo-ngernkham T, Li LY, Damrongwiriyanupap N, Chindaprasirt P. Strength development and durability of alkali-activated fly ash mortar with calcium carbide residue as additive. Constr Build Mater. 2018;162:714-23.
[7]   Songpiriyakij S, Pulngern T, Pungpremtrakul P, Jaturapitakkul C. Anchorage of steel bars in concrete by geopolymer paste. Mater Des. 2011;32(5):3021-8.
[8]   Sarker PK. Bond strength of reinforcing steel embedded in fly ash-based geopolymer concrete. Mater Struct. 2011;44(5): 1021-30.
[9]   Sarker PK, Kelly S, Yao Z. Effect of fire exposure on cracking, spalling and residual strength of fly ash geopolymer concrete. Mater Des. 2014;63:584-92.
[10] Phoo-ngernkham T, Hanjitsuwan S, Damrongwiriyanupap N, Chindaprasirt P. Effect of sodium hydroxide and sodium silicate solutions on strengths of alkali activated high calcium fly ash containing Portland cement. KSCE J Civ Eng. 2017;21(6): 2202-10.
[11] Phoo-ngernkham T, Hanjitsuwan S, Li LY, Damrongwiriyanupap N, Chindaprasirt P. Adhesion characterization of Portland cement concrete and alkali-activated binders under different types of calcium promoters. Adv Cem Res. 2019;31(2):69-79.
[12] Phoo-ngernkham T, Sata V, Hanjitsuwan S, Ridtirud C, Hatanaka S, Chindaprasirt P. High calcium fly ash geopolymer mortar containing Portland cement for use as repair material. Constr Build Mater. 2015;98:482-8.
[13] Sukontasukkul P, Chindaprasirt P, Pongsopha P, Phoo-Ngernkham T, Tangchirapat W, Banthia N. Effect of fly ash/silica fume ratio and curing condition on mechanical properties of fiber-reinforced geopolymer. J Sustain Cement Base Mater. 2020:4(1): 1-15.
[14] Pacheco-Torgal F, Castro-Gomes J, Jalali S. Alkali-activated binders: a review. Part 1. Historical background, terminology, reaction mechanisms and hydration products. Constr Build Mater. 2008;22(7):1305-14.
[15] Li C, Sun H, Li L. A review: the comparison between alkali-activated slag (Si+Ca) and metakaolin (Si+Al) cements. Cem Concr Res. 2010;40(9):1341-9.
[16] Hanjitsuwan S, Injorhor B, Phoo-ngernkham T, Damrongwiriyanupap N, Li LY, Sukontasukkul P, et al. Drying shrinkage, strength and microstructure of alkali-activated high-calcium fly ash using FGD-gypsum and dolomite as expansive additive. Cem Concr Compos. 2020;114:103760.
[17] Phoo-ngernkham T, Phiangphimai C, Intarabut D, Hanjitsuwan S, Damrongwiriyanupap N, Li LY, et al. Low cost and sustainable repair material made from alkali-activated high-calcium fly ash with calcium carbide residue. Constr Build Mater. 2020;247:118543.
[18] Ridtirud C, Chindaprasirt P, Pimraksa K. Factors affecting the shrinkage of fly ash geopolymers. Int J Miner Metall Mater. 2011;18(1):100-4.
[19] Punurai W, Kroehong W, Saptamongkol A, Chindaprasirt P. Mechanical properties, microstructure and drying shrinkage of hybrid fly ash-basalt fiber geopolymer paste. Constr Build Mater. 2018;186:62-70.
[20] Matalkah F, Salem T, Shaafaey M, Soroushian P. Drying shrinkage of alkali activated binders cured at room temperature. Constr Build Mater. 2019;201:563-70.

[21] Bakharev T, Sanjayan JG, Cheng YB. Effect of admixtures on properties of alkali-activated slag concrete. Cem Concr Res. 2000;30(9):1367-74.

[22] ASTM. ASTM C618-15, Standard specification for coal fly ash and raw or calcined natural pozzolan for use in concrete. West Conshohocken: ASTM International; 2015.

[23] ASTM. ASTM C191-13, Standard test method for time of setting of hydrualic cement by vicat needle. West Conshohocken: ASTM International; 2013.

[24] ASTM. ASTM C109, Standard test method of compressive strength of hydrualic cement mortars (using 2-in. or [50 mm] cube specimens). West Conshohocken: ASTM International; 2002.

[25] ASTM. ASTM C490, Standard practice for use of apparatus for the determination of length change of hardened cement paste, mortar, and concrete. West Conshohocken: ASTM International; 2017.

[26] ASTM. ASTM C596. Standard test method for drying shrinkage of mortar containing hydraulic cement. West Conshohocken: ASTM International; 2017.

[27] Pangdaeng S, Phoo-ngernkham T, Sata V, Chindaprasirt P. Influence of curing conditions on properties of high calcium fly ash geopolymer containing Portland cement as additive. Mater Des. 2014;53:269-74.

[28] Chindaprasirt P, De Silva P, Sagoe-Crenstil K, Hanjitsuwan S. Effect of SiO_2 and Al_2O_3 on the setting and hardening of high calcium fly ash-based geopolymer systems. J Mater Sci. 2012;47(12):4876-83.

[29] Hanjitsuwan S, Phoo-ngernkham T, Damrongwiriyanupap N. Comparative study using portland cement and calcium carbide residue as a promoter in bottom ash geopolymer mortar. Constr Build Mater. 2017;133:128-34.

[30] Wu H, Zhu M, Liu Z, Yin J. Developing a polymer-based crack repairing material using interpenetrate polymer network (IPN) technology. Constr Build Mater. 2015;84:192-200.

[31] Chindaprasirt P, Thaiwitcharoen S, Kaewpirom S, Rattanasak U. Controlling ettringite formation in FBC fly ash geopolymer concrete. Cem Concr Compos. 2013;41:24-8.

[32] Boonserm K, Sata V, Pimraksa K, Chindaprasirt P. Improved geopolymerization of bottom ash by incorporating fly ash and using waste gypsum as additive. Cem Concr Compos. 2012;34(7):819-24.

[33] Ma W, Brown PW. Hydrothermal reactions of fly ash with $Ca(OH)_2$ and $CaSO_4.2H_2O$. Cem Concr Res. 1997;27(8):1237-48.

[34] Yusuf MO, Megat Johari MA, Ahmad ZA, Maslehuddin M. Shrinkage and strength of alkaline activated ground steel slag/ultrafine palm oil fuel ash pastes and mortars. Mater Des. 2014;63:710-8.

[35] Guo X, Shi H, Chen L, Dick WA. Alkali-activated complex binders from class C fly ash and Ca-containing admixtures. J Hazard Mater. 2010;173(1-3):480-6.

[36] Guo X, Shi H, Dick WA. Compressive strength and microstructural characteristics of class C fly ash geopolymer. Cem Concr Compos. 2010;32(2):142-7.